# SC/69A/ASI/01 Rev

**Sub-committees/working group name:**

**Capture-recapture estimates of abundance of Antarctic blue whales**

**Paula A. Olson, Douglas Kinzey, Michael C. Double, Koji Matsuoka, Ken Findlay**

INTERNATIONAL
WHALING COMMISSION

Papers submitted to the IWC are produced to advance discussions within that meeting; they may be preliminary or exploratory.

It is important that if you wish to cite this paper outside the context of an IWC meeting, you notify the author at least six weeks before it is cited to ensure that it has not been superseded or found to contain errors.

# Capture-recapture estimates of abundance of Antarctic blue whales

Paula A. Olson[1], Douglas Kinzey[1], Michael C. Double[2], Koji Matsuoka[3], Ken Findlay[4]

[1]Southwest Fisheries Science Center, NMFS/NOAA, 8901 La Jolla Shores Drive, La Jolla, CA 92037 USA
[2]Antarctic Ecosystem Research Division, Australian Marine Mammal Centre, Australian Antarctic Division, 203 Channel Highway, Kingston, Tasmania 7001 Australia
[3]Institute of Cetacean Research, Toyomi-cho 4-5, Chuo-ku Tokyo 104-0055, Japan
[4]Mammal Research Institute Whale Unit, University of Pretoria. [c/o Iziko SA Museum, PO Box 61, Cape Town 8000, South Africa]

*Paula.Olson@noaa.gov*

**ABSTRACT**
Photo-identification data of Antarctic blue whales from 2003/2004 to 2018/2019 were used in a capture-recapture analysis to produce estimates of population abundance and growth rate for the circumpolar Antarctic. Photographs were collected during IWC-SOWER, IWC-SORP, ICR, and SAABWS cruises and also made available by opportunistic contributors. Separate capture-recapture estimates were made using photos taken of the right and left sides of the whales. Two capture-recapture models, POPAN and Pradel, were applied to these data to estimate superpopulation abundance (N), recruitment-immigration (pent), and probability of capture (p) from the POPAN model and probability of capture and population growth rate (lambda) from the Pradel model. The fits of a series of pre-specified apparent survival rates from 0.75 to 1 were compared using ΔAICc. Derived parameters of annual abundances and population growth rate were calculated from the POPAN models. A wide range of annual survival rates were consistent with the capture-recapture data based on ΔAICc scores. Four different best-fitting configurations of left side data, right side data, POPAN, and PradLambda had survival rates of 0.94, 0.87, 0.97 and 0.9 (mean 0.92). The best superpopulation estimates from POPAN for the left and right sides were 3,488 (95% CI = 1754, 7178) and 3,659 (95% CI = 1906, 7241) whales, respectively. Assigning a survival rate of 0.92 to the combined and right and left side models produced an abundance estimate for the last year, 2018/2019 (2,050 whales ; CI = 1,135 to 3,704) that was lower than the projected abundance for 2019 from Branch (2004) (9,608 whales (CI = 1257 to 26,060 whales)). Assigning a higher survival rate of 0.99 for the POPAN models produced higher annual estimates of abundance although still less than the projections from Branch (2004). Population growth rates from Pradel, POPAN and Branch (2007) were also compared. Estimated population growth rates from the Pradel and POPAN models during 2003/2004 – 2018/2019 were at the upper end of the Branch (2007) growth estimates for 1997/1998. The Pradel and POPAN models suggested annual population growth was slowing by the end of the time series instead of increasing exponentially.

KEYWORDS: ANTARCTIC, PHOTO-ID, MARK-RECAPTURE, ABUNDANCE ESTIMATE

## INTRODUCTION
During the first half of the 20th Century, the population of Antarctic blue whales (*Balaenoptera musculus intermedia)* was reduced by whaling from an estimated pre-exploitation size of 239,000 (95% CI=202,000-311,000) to less than 1% of its former abundance (Branch, 2007). To date the population has not recovered to its pre-exploitation size, although Branch *et al.* (2004) provides evidence that the population is increasing. Antarctic blue whales are listed as Critically Endangered by the International Union for the Conservation of Nature (Reilly *et al*., 2008). In 2006 the IWC Scientific Committee initiated an in-depth assessment of this population and Branch (2007) produced estimates of abundance from each of the three circumpolar sets of surveys[1] conducted under the IWC IDCR/SOWER[2] program. Branch's (2007) work provides the most recent population abundance estimate accepted by the IWC, 2,280 (CV=0.36), and is based on data from the last IDCR/SOWER circumpolar series, CPIII. The estimate was based on the CPIII midpoint year 1997/1998. Currently the Scientific Committee is planning a new in-depth assessment of this population (IWC, 2022).

[1] CPI (1978/79-1983/84), CPII (1985/86-1990/91), CPIII (1991/92-2003/04)

[2] International Decade of Cetacean Research/Southern Ocean Whale Ecosystem Research

The Antarctic Blue Whale Catalogue (Olson *et al*., 2020) contains photo-identification data available for analysis in a capture-recapture estimate of abundance. Previously we conducted capture-recapture estimates with these data (Olson *et al*. 2018; 2021), and in addressing comments from the Committee in response to those estimates we have reworked the analysis here. We used right and left side photographs to calculate separate circumpolar estimates for the number of blue whales present from 2003/2004 to 2018/2019.

## METHODS

### Field methods

Research cruises conducted by year are given in Table 1. During IWC-SOWER and ICR[3] cruises, photo-identification effort was conducted ancillary to the primary cruise objectives, thus the amount of effort varied by year (Matsuoka *et al.*, 2003; Matsuoka and Pastene, 2009; Olson, 2010). Photo-ID was most often conducted from the bow of the research vessel in conjunction with biopsy sampling. Blue whale research was the primary objective of the IWC-SORP and SAABWS[4] voyages where photo-ID was also conducted in conjunction with biopsy sampling (Double *et al.*, 2013; Double *et al.*, 2015; Double *et al.*, 2021; Findlay, *et al.* 2014). The 2013 IWC-SORP voyage operated an inflatable boat for approaches as well as the larger ship.

Both right and left sides of the whales were photographed whenever possible, but not all whales were approachable on both sides. 35mm SLR cameras using black and white film were used through 2004/2005, overlapping in use with digital SLR cameras beginning in 2003/2004. Digital SLR cameras were used exclusively starting with the 2005/2006 season. Cameras had zoom lenses with maximum focal lengths ranging from 200-400mm.

### Photo-ID data

Digital SLR cameras substantially improved the quality of identification photographs and resulted in larger sample sizes starting in 2003/2004. Previous explorations of the photo-ID data including the earlier years with film photographs (1990/1991 – 2002/2003) resulted in capture-recapture models with problems of convergence and extremely high uncertainty in the estimates for annual abundances in the earliest years (Olson *et al*., 2018; 2021). Therefore, the time period 2003/2004 – 2018/2019 was selected for the analysis here.

Identification photographs of Antarctic blue whales were available from 6 IWC-SOWER cruises, 3 IWC-SORP voyages, 10 ICR cruises, and 1 SAABWS voyage from a 16-year period, 2003/2004 through 2018/2019. The IWC-sponsored Southern Hemisphere Blue Whale Catalogue (Galletti Vernazzani *et al*., 2022) facilitated the collaborative use of photographs. Photographs that were collected opportunistically by scientists working on other projects in the Antarctic and from citizen scientists aboard tourist vessels were also made available to the catalogue. Good quality opportunistic photographs come from six seasons 2009/2010 through 2018/2019.

Photographs from all sources were obtained during the Austral summer.

Antarctic blue whale photographs were examined for unique natural markings and identified as individuals following methods outlined in Gendron and Ugalde de la Cruz (2012) and Sears *et al.* (1990). The methods required the presence of the dorsal fin in the photo. Identification photos were selected for each whale, an identification number assigned, and the photos compiled into a photo-ID catalogue. (Identifications from the ICR and SAABWS photo collections were cross-referenced.) Identification photographs were compared within and between years. The Antarctic Blue Whale Photo-identification Catalogue is maintained at the Southwest Fisheries Science Center in the USA (Olson, 2010).

Identification photos (the best right side and best left side for each individual whale) were coded for quality using a four-tier system representing photo quality ranging from excellent (code 1) to poor (code 4) (Olson *et al*., 2021). Photo quality was based on three features: angle to the subject, exposure and focus. Photos with the top three codes were used in capture-recapture analysis (and weighted equally).

[3] Institute of Cetacean Research

[4] South African Antarctic Blue Whale Survey

**Capture-recapture analysis**

Given the uncertainty of population identity of blue whales north of 60°S, only photographs obtained south of 60°S were used in the analysis. All Antarctic blue whales were treated as a single population assumed to mix freely throughout the Southern Ocean south of 60°S. Individual Antarctic blue whales have been documented to move at least 6,550km within the Southern Ocean between inter-annual re-sightings (Olson *et al*., 2016).

Each research season (year) was considered a sampling occasion. The database is an array of ones and zeros indicating the number of individuals identified (rows) by the number of sampling occasions (columns). Thus, each row represents an identified individual with a "1" in the occasion(s) it was sighted and a "0" during sampling occasions when that individual was not sighted. Within-year re-sightings were ignored.

Capture-recapture modeling was conducted using the R package 'RMark' version 3.0.0 (Laake and Rexstad, 2011) as an interface to the program 'Mark' version 10.0 (Cooch and White, 2011). Two open-population implementations of the Jolly-Seber model, POPAN and PradLambda, were applied to the capture-recapture data for each side. These models allow births, deaths, immigration and emigration during the time period of the study. POPAN can estimate four population parameters: apparent survival (***Phi***) (this can include emigration); the probability of capture (***p***) given that an individual is present; the probability of entry (***pent***), which can be a combination of recruitment and immigration; and the superpopulation (***N***), the total number of individuals estimated to be present during the period of sampling. In the POPAN model the first year value of pent is derived as 1-sum (estimated pents from all subsequent years), with a MLogit link function insuring that the sum of the pent values for all years equals one. Derived estimates of the annual numbers of individual whales can be calculated once these four estimated parameters are obtained from POPAN. We estimated the population growth rate from 2003/2004 to 2018/2019 from the first and last of these annual abundances as:

$$(N_t/N_0)^{1/n_t} - 1$$

where

$N_t$ is abundance in 2018/2019, the final year,

$N_0$ is abundance in 2003/2004, the first year,

$n_t$ is the number of years (15) when $N_0$ = 2003/2004.

PradLambda is a variant of the Pradel capture-recapture model that estimates three parameters: ***Phi***, ***p*** and ***Lambda (λ)***. Phi and p represent survival and probability of capture as described above. Lambda is the realized population growth rate. Unlike the POPAN model, the Pradel model estimates growth rate as a proportion without estimating abundance.

Initial trials supplying the blue whale capture-recapture data to POPAN and PradLambda models indicated that not all parameters were simultaneously identifiable. A series of models representing the right and left side photos was therefore supplied with pre-specified survival rates, Phi, from 0.75 to 1. The p, pent, N and $\lambda$ parameters were then estimated from the POPAN and PradLambda models for the right and left side survival series, and the best of the two models for each side and Phi value were chosen using the $\Delta AIC_c$ score. The best four models for each of these configurations (left POPAN, right POPAN, left PradLambda, right PradLambda) were identified based on these comparisons.

The mean of the four survival rates from the best model-data configurations was calculated. The estimates of models using this mean Phi were compared to the estimates from the models with the best Phi value for the individual model and data configurations. The growth rate calculated from the POPAN abundances was compared to the Pradel estimate of Lambda.

The right and left side sample sizes in the capture-recapture POPAN estimates were similar (right side = 225 whales, left side = 214 whales). For comparison with the Branch projections for 2003/2004 – 2018/2019, annual mean abundances $(\widehat{N})$ and variances $\left(Var(\widehat{N})\right)$ were calculated for the combined left and right sides using inverse-variance weightings as $\widehat{N} = \frac{\sum_i N_i/\sigma_i^2}{\sum_i 1/\sigma_i^2}$ and $Var(\widehat{N}) = \frac{1}{\sum_i 1/\sigma_i^2}$, where side is indexed by $i$.

The CV for the combined sides was:

$$\text{CV} = e^{\left(1.96\sqrt{ln\left((1+(\text{SE}(N_t)/N_t)^2)\right)}\right)}$$

where
$N_t$ = the annual abundance estimates for the combined sides,
SE$(N_t)$ = the standard errors of annual abundances for the combined sides.

The combined lower and upper confidence intervals were calculated as:

$$95\%\ \text{CI}=(N_t/CV, N_t\ CV).$$

where
$N_t$ = the mean of the right and left side abundance estimates,
CV = the combined CV.

**RESULTS**

**Photo-ID**

For the time period 2003/2004 – 2018/2019, 225 right side and 214 left side individual blue whale photos met the criteria for the top three quality codes (Table 1), with 12 recaptures for the right side and 10 recaptures for the left side (Table 2). Whales were photo-identified in all six IWC Management Areas.

**Table 1**. Numbers by year of left and right side Antarctic blue whale identification photographs, 2003/2004 – 2018/2019, quality codes 1-3, used in the capture-recapture analyses. (Photographs of recaptured whales appear more than once.) Opportunistic = photos contributed from collegial and citizen scientists.

| Season | No. left side photos | No. right side photos | Source |
|---|---|---|---|
| 2003/2004 | 5 | 9 | IWC |
| 2004/2005 | 12 | 7 | IWC, ICR |
| 2005/2006 | 31 | 29 | IWC, ICR |
| 2006/2007 | 58 | 65 | IWC, ICR |
| 2007/2008 | 7 | 3 | IWC, ICR |
| 2008/2009 | 9 | 8 | IWC, ICR |
| 2009/2010 | 4 | 7 | ICR, opportunistic |
| 2012/2013 | 32 | 33 | IWC-SORP, ICR |
| 2013/2014 | 6 | 4 | SAABWS, opportunistic |
| 2014/2015 | 24 | 29 | IWC-SORP, ICR, opportunistic |
| 2015/2016 | 15 | 13 | ICR, opportunistic |
| 2016/2017 | 4 | 3 | ICR |
| 2017/2018 | 1 | 4 | opportunistic |
| 2018/2019 | 16 | 21 | IWC-SORP, opportunistic |

**Table 2**. Recaptured Antarctic blue whales, 2004/2005 – 2018/2019.

| Whale ID | Side | Capture season | Recapture season | Interval (years) |
|---|---|---|---|---|
| 0622 | left | 2006 | 2007 | 1 |
| 0623 | left | 2006 | 2007 | 1 |
| 0761 | left | 2005 | 2007 | 2 |
| 0607 | left | 2006 | 2008 | 2 |
| 0738 | left | 2007 | 2010 | 3 |
| 0802 | left | 2008 | 2013 | 5 |
| 0758 | left | 2007 | 2013 | 6 |
| 1306 | left | 2013 | 2019 | 6 |
| 1313 | left | 2006 | 2013 | 7 |
| 1322 | left | 2006 | 2013 | 7 |
| 0623 | right | 2005 | 2006 | 1 |
| 0623 | right | 2006 | 2007 | 1 |
| 0622 | right | 2006 | 2007 | 1 |
| 0761 | right | 2005 | 2007 | 2 |
| 1343 | right | 2013 | 2015 | 2 |
| 0104 | right | 2001 | 2004 | 3 |
| 1005 | right | 2010 | 2013 | 3 |
| 0802 | right | 2008 | 2013 | 5 |
| 0758 | right | 2007 | 2013 | 6 |
| 1313 | right | 2006 | 2013 | 7 |
| 1322 | right | 2006 | 2013 | 7 |
| J062 | right | 2003 | 2015 | 12 |

**Capture-recapture**
Most of the four model series' of configurations with pre-specified survival values from 0.75 to 1 were within 2 $\Delta AIC_c$ of one another, indicating the wide range of plausible survival values consistent with these capture-recapture data (**Figure 1, Supplementary Tables 1 to 4**). The best-fitting (lowest $\Delta AIC_c$) of the four model combinations of left side data, right side data, POPAN, and PradLambda were at four different survival values: 0.94, 0.87, 0.97 and 0.9 (left side POPAN, right side POPAN, left side PradLambda, and right side PradLambda, respectively). The mean of these four values of survival was 0.92 (95% CI = 0.83, 1). The corresponding best superpopulation estimates from POPAN for the left and right sides were 3,488 (95% CI = 1754, 7178) and 3,659 (95% CI = 1906, 7241) whales, respectively.

The realized population growth rates from the best PradLambda models were 1.13 (95% CI = 0.98, 1.31) from the left side (best Phi = 0.97) and 1.14 (95% CI = 0.98, 1.131) for the right side (best Phi = 0.9) (**Figure 2**). After adding 1 to compound growth rates to make them comparable with Lambda rates, the POPAN derived mark-recapture growth rates were 1.10 (left) and 1.13 (right). The comparable growth rate from Branch (2007) was 1.0 + 0.082 = 1.082 (95% CI = 1.016, 1.148). Thus the POPAN and Pradel growth rates were near the upper limit of the Branch (2007) confidence interval for population growth rate.

Derived values of the annual abundances from the POPAN models with different best-fitting Phi values for each side (0.94 left, 0.87 right)) (**Figure 3A, Supplementary Tables 5, 6**) and the mean Phi value of 0.92 (**Figure 3B, Supplementary Tables 7, 8**) produced similar patterns of increasing abundance from 2004 to 2019 from the two data sets.

The best POPAN models for both the right and left sides estimated a time-constant probability of entry (pent) of 0.06 for each of the years 2004/2005 – 2018/2019. The pent value for year 2003/2004 was derived as 1-sum(15*0.06) = 0.1, making the sum of the 16 years of pent estimates equal to 1.

The 1998 abundance estimates from Branch (2004) projected forward to 2003/2004 – 2018/2019 were higher than the capture-recapture estimates for the same period (**Figure 4**).The Branch projection for the mean population size in 2018/2019 was 9,608 whales (CI = 1257, 26,060). The left and right side combined capture-recapture abundance in 2018/2019 was 2,050 whales (CI = 1135, 3704) when survival was 0.92 (**Figure 4A**). When survival was increased to 0.99 the combined capture-recapture estimates increased to 3,683 whales, with overlapping confidence intervals during the last half of the projection period (**Figure 4B, Supplementary Tables 11, 12**).

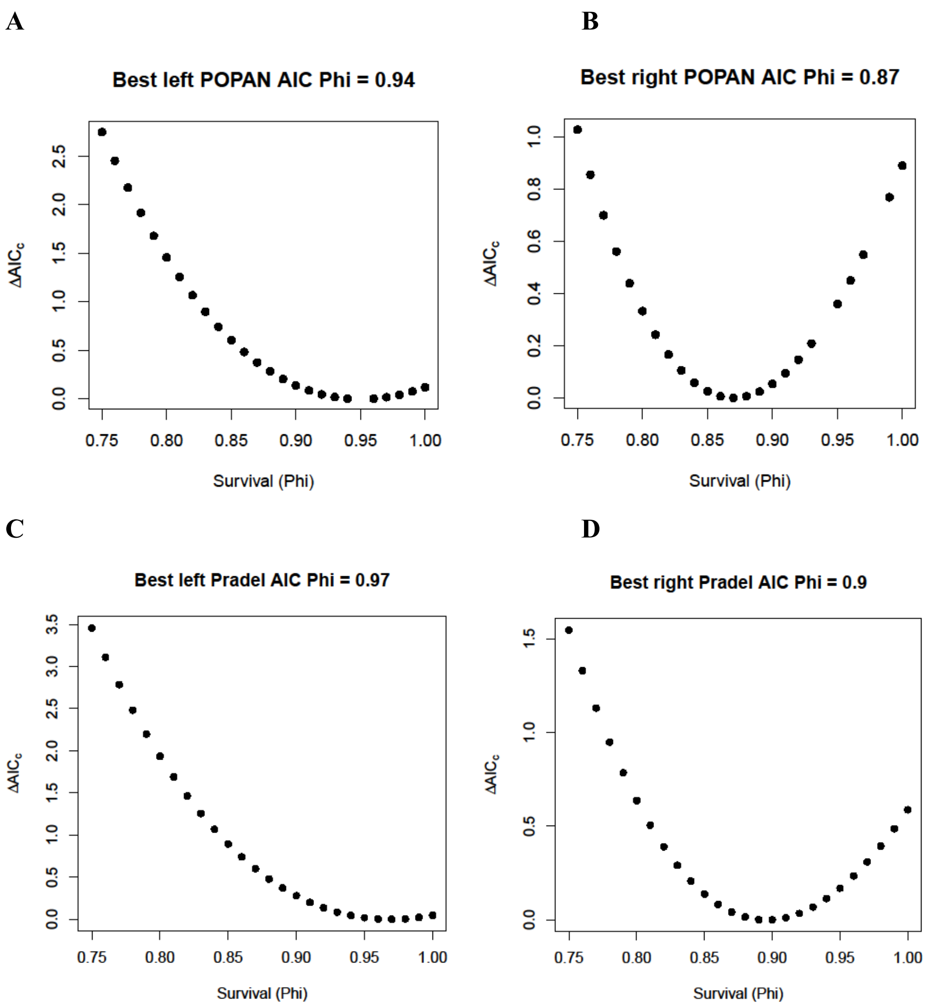


**Figure 1**. $\Delta AIC_c$ scores of capture-recapture configurations with pre-specified Phi (survival) values for: **A** left side POPAN; **B** right side POPAN; **C** left side Pradel and **D** right side Pradel models. Missing sections in the POPAN plots represent model non-convergence or $\Delta AIC_c$ scores greater than 3.5 at those Phi values.

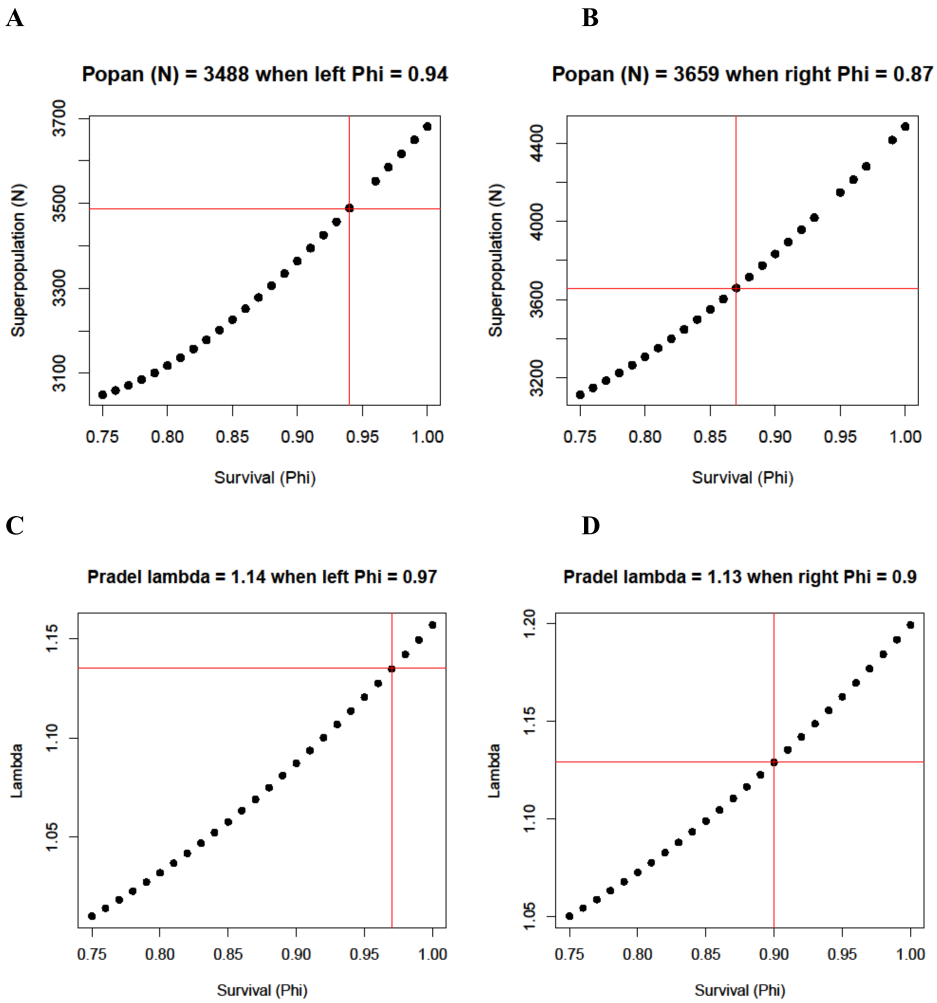


**Figure 2**. Capture-recapture estimates using pre-specified survivals (Phi) for: **A** the superpopulation (N) from left side POPAN; **B** the superpopulation (N) from right side POPAN; **C** the finite population growth rate Lambda (λ) from left side Pradel; **D** the finite growth rate from right side Pradel models. Red lines indicate the best $\Delta AIC_c$-selected models.

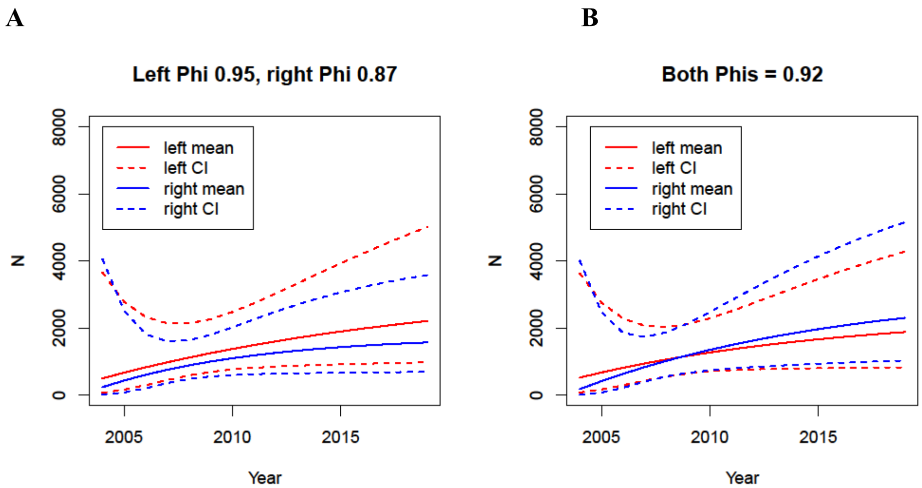


**Figure 3**. Means and confidence intervals of left side (red) and right side (blue) estimates of annual abundance of Antarctic blue whales derived from POPAN models using (**A**) the best $\Delta AIC_c$-selected left and right side specific Phi values of 0.95 and 0.87, respectively, and (**B**) mean Phi values of 0.92 for both left and right sides.

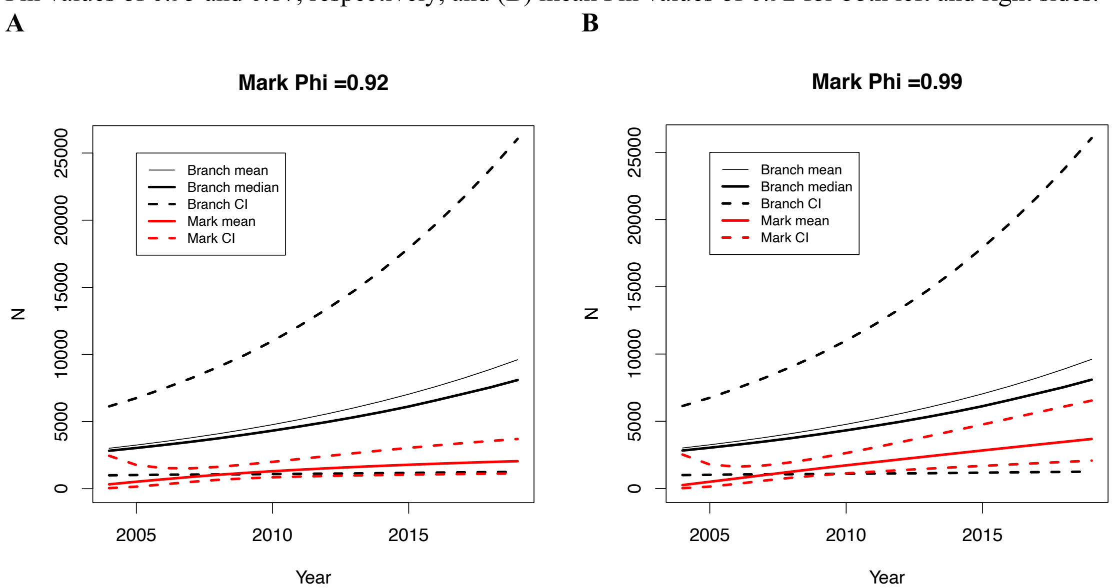


**Figure 4**. Means and confidence intervals of annual abundance estimates for Antarctic blue whales for 2003/2004 – 2018/2019 projected from Branch (2004) estimates (black) and from the combined left and right side mark-recapture models with (**A)** apparent survival = 0.92 and (**B**) apparent survival = 0.99.

## DISCUSSION

Capture-recapture estimates using photo-ID data of population scale and trends provide an alternative, lower estimate of the population size of Antarctic blue whales for 2003/2004 – 2018/2019 to projections from the Branch (2004) estimates for 1997/1998. Without additional line-transect and photo-ID surveys these differences may be difficult to resolve. One option for current management could be to combine the 1997/1998 projections from Branch (2007) with the 2003/2004 – 2018/2019 mark-recapture estimates analogously as was implemented in this study for the right and left side photo-ID estimates. Use of prior distributions in a Bayesian approach using these capture-recapture data is another option.

Although the population growth rates of 13-14% estimated by the best Pradel models and 10-13% derived from the best POPAN models were greater than the 8.2% estimated by Branch (2007), examination of the POPAN annual abundances (**Figures 3, 4; Supplementary Tables 5-8**) show even higher growth rates at the start of the time series, with decreasing growth in the latter portion of the series. POPAN-derived growth rates from 2003/2004 to 2004/2005 exceeded 50% in some cases, a biologically implausible rate.

The life span of blue whales is 80-90 years (Sears and Perrin, 2018). Beyond their potential use in estimating the current abundance of the population, some of the individual Antarctic blue whales identified in this study will continue to be recognizable in future decades. The Antarctic blue whale photo-id database will enable these individuals to be re-identified in future studies of population abundance, movement and behavior.

**ACKNOWLEDGEMENTS**
Bob Brownell was instrumental in facilitating photo-ID analysis. We thank him, and thank Jeff Laake for his guidance on capture-recapture analysis. Paul Ensor's vision and advice made this work possible. Trevor Branch kindly provided the projections from his 2007 paper. Warm thanks to the captains, crews and scientists aboard all of the research vessels. We are grateful to the many people who generously contributed their personal photos. Special thanks to Ted Cheeseman and happywhale.com. Support was allocated to the author (PAO) at SC58, SC61, SC64, SC65, SC66B for the analysis Antarctic blue whale photographs.

**REFERENCES**
Branch, T.A. 2007. Abundance of Antarctic blue whales south of 60°S from three complete circumpolar sets of surveys. *J. Cetacean Res. Manage.* 9: 87–96.

Branch, T.A., Matsuoka, K. and Miyashita, T. 2004. Evidence for increases in Antarctic blue whales based on Bayesian modelling. *Mar. Mammal Sci.* 20(4): 726-54.

Cooch, E. and White, G. (eds.). 2011. Program MARK: A Gentle Introduction. 9th Edition. Available at: http://www.phidot.org/software/mark/docs/book/.

Double, M.C., Barlow, J., Miller, B.S., Olson, P., Andrews-Goff, V., Leaper, R., Ensor, P., Kelly, N., Wadley, V., Lindsay, M., Peel, D., Calderan, S., Collins, K., Davidson, M., Deacon, C., Donnelly, D., Olavarria, C., Owen, K., Rekdahl, M., Schmitt, N. and Gales, N. 2013. Cruise report of the 2013 Antarctic blue whale voyage of the Southern Ocean Research Partnership. Paper SC/65a/SH21 submitted to the IWC Scientific Committee.

Double, M.C., Bell, E., Miller, B., Kelly, N., Kawaguchi, S., Lawrence, J., Leaper, R., Olson, P., Westwood, K., Andrews-Goff, V., Boyd, C., Calderan, S., Donnelly, D., Holmes, T., Irvine, L., Johnson, O., Kavanagh, A., King, R., Melvin, J., Miller, E., O'Brien, J., Ratnarajah, L., Reyes Reyes, V., Rodriguez Vives, C., Širović, A., Smith, A., Stafford, K., and Zhang, H. 2021. ENRICH Voyage Report, IN2019_V01: The availability of Antarctic krill to large predators and their role in biogeochemical recycling in the Southern Ocean. Australian Antarctic Division. Paper SC/68c/ submitted to the IWC Scientific Committee.

Double, M.C., Miller, B.S., Leaper, R., Olson, P., Cox, M.J., Miller, E., Calderan, S., Collins, K., Donnelly, D., Ensor, P., Goetz, K., Schmitt, N., Andrews-Goff, V., Bell, E. and O'Driscoll, R. 2015. Cruise report on blue whale research from the NZ/Australia Antarctic Ecosystems Voyage 2015 of the Southern Ocean Research Partnership. Paper SC/66a/SH7 submitted to the IWC Scientific Committee.

Findlay, K., Thornton, M., Shabangu, F., Venter, K., Thompson, I., and Fabriciussen, O. 2014. Report of the 2013/2014 South African Antarctic Blue Whale Survey, 000°-020°E. Paper SC/65b/SH01 submitted to the IWC Scientific Committee.

Galletti Vernazzani, B., Jackson, J.A., Cabrera, E., Carlson, C.A., Brownell, R.L., Jr. 2017. Estimates of abundance and trend of Chilean blue whales off Isla de Chiloe´, Chile. PLoS ONE 12(1): e0168646.

Galletti Vernazzani, Olson, PA, Salgado-Kent, C. 2022. Progress report on Southern Hemisphere Blue Whale Catalogue: Period April 2021- March 2022. SC/68D/SH/04.

Gendron, D. and Ugalde de la Cruz, A. 2012. A new classification method to simplify blue whale photo-identification technique. *J. Cetacean Res. Manage.* 12: 79-84.

IWC. 2022. Report of the Scientific Committee SC68D. Available from https://iwc.int/

Laake, J. and Rexstad, E. 2011. RMark - an alternative approach to building linear models in MARK. Appendix C of: Cooch, Evan and Gary White (eds). Program MARK: A Gentle Introduction. 9th Edition. Available at: http://www.phidot.org/software/mark/docs/book/.

Matsuoka, K., P. Ensor, T. Hakamada, H. Shimada, S. Nishiwaki, F. Kasamatsu, and H. Kato. 2003. Overview of minke whale sightings surveys conducted on IWC/IDCR and SOWER Antarctic cruises from 1978/79 to 2000/01. *J. Cetacean. Res. Manage*. 5(2):173-201.

Matsuoka, K., and Pastene, L. 2009. Summary of photo-id information of blue whales collected by JARPA/JARPA II and preliminary analysis of matches in the feeding grounds. Paper SC/61/SH3 submitted to the IWC Scientific Committee.

Olson, P.A. 2010. Blue whale photo-identification from IWC IDCR/SOWER cruises 1987/1988 to 2008/2009. Paper SC/62/SH29 presented to the IWC Scientific Committee.

Olson, P.A., Double, M.C., Matsuoka, K., and Pastene, L.A., Findlay, K. 2020. The Antarctic Blue Whale Catalogue: new data from 2015-2019. Paper submitted to the IWC Scientific Committee. SC/68B/PH04.

Olson, P.A., Galletti Vernazzani, B., Torres Florez, J.P. 2021. Southern Hemisphere Blue Whale Catalogue photo quality coding guide. SC/68C/PH02.

Olson, P.A., Kinzey, D., Double, M.C., Matsuoka, K., Pastene, L.A. and Findlay, K. 2018. Capture-recapture estimates of abundance of Antarctic blue whales. Paper SC/67B/SH08 submitted to the IWC Scientific Committee.

Olson, P.A., Kinzey, D., Double, M.C., Matsuoka, K., Findlay, K. 2021. Capture-recapture estimates of abundance of Antarctic blue whales. Paper SC/68C/ASI15 submitted to the IWC Scientific Committee.

Reilly, S.B., Bannister, J.L., Best, P.B., Brown, M., Brownell Jr., R.L., Butterworth, D.S., Clapham, P.J., Cooke, J., Donovan, G.P., Urbán, J. and Zerbini, A.N. 2008. *Balaenoptera musculus ssp. intermedia*. The IUCN Red List of Threatened Species 2008: e.T41713A10543676.

Sears, R. and Perrin, W.F. Blue whale (*Balaenoptera musculus*). In Encyclopedia of Marine Mammals, 3rd Edition. Eds. B. Würsig, J.G.M. Thewissen, and K. Kovacs. San Diego: Academic Press/Elsevier.

Sears, R., Williamson, J.M, Wenzel, F.W., Bérubé, M., Gendron, D. and Jones, P. 1990. Photographic identification of the blue whale (*Balaenoptera musculus*) in the Gulf of St. Lawrence, Canada. *Rep. Int. Whal. Commn*., (Special Issue) 12: 335-342.

**Supplementary Table 1**. Left side POPAN model estimates of the superpopulation (N) from configurations supplied with pre-specified survival rates (Phi) from 0.75 to 1 and the associated $AIC_c$ and $\Delta AIC_c$ scores.

| Phi | N | AICc | deltaAICc |
|---|---|---|---|
| 0.75 | 3049 | 201.1203 | 2.74437 |
| 0.76 | 3059 | 200.8249 | 2.44892 |
| 0.77 | 3071 | 200.5486 | 2.17259 |
| 0.78 | 3085 | 200.2909 | 1.91498 |
| 0.79 | 3101 | 200.0517 | 1.67573 |
| 0.8 | 3118 | 199.8304 | 1.45443 |
| 0.81 | 3136 | 199.6267 | 1.25069 |
| 0.82 | 3157 | 199.4401 | 1.0641 |
| 0.83 | 3179 | 199.2702 | 0.89423 |
| 0.84 | 3202 | 199.1166 | 0.74066 |
| 0.85 | 3226 | 198.9789 | 0.60295 |
| 0.86 | 3252 | 198.8566 | 0.48065 |
| 0.87 | 3278 | 198.7493 | 0.3733 |
| 0.88 | 3306 | 198.6564 | 0.28042 |
| 0.89 | 3335 | 198.5775 | 0.20155 |
| 0.9 | 3364 | 198.5122 | 0.13619 |
| 0.91 | 3394 | 198.4598 | 0.08385 |
| 0.92 | 3425 | 198.42 | 0.04404 |
| 0.93 | 3456 | 198.3922 | 0.01626 |
| 0.94 | 3488 | 198.376 | 0 |
| 0.95 | 2586 | 202.7361 | 4.36015 |
| 0.96 | 3552 | 198.376 | 7.00E-05 |
| 0.97 | 3585 | 198.3914 | 0.01541 |
| 0.98 | 3617 | 198.4163 | 0.0403 |
| 0.99 | 3650 | 198.4502 | 0.07425 |
| 1 | 3680 | 198.4928 | 0.11681 |

**Supplementary Table 2**. Right side POPAN model estimates of the superpopulation (N) from configurations supplied with pre-specified survival rates (Phi) from 0.75 to 1 and the associated $AIC_c$ and $\Delta AIC_c$ scores.

| Phi | N | AICc | deltaAICc |
|---|---|---|---|
| 0.75 | 3115 | 190.0697 | 1.02816 |
| 0.76 | 3150 | 189.8972 | 0.85568 |
| 0.77 | 3186 | 189.7419 | 0.70031 |
| 0.78 | 3225 | 189.6032 | 0.56166 |
| 0.79 | 3266 | 189.4809 | 0.43936 |
| 0.8 | 3309 | 189.3745 | 0.333 |
| 0.81 | 3354 | 189.2837 | 0.24217 |
| 0.82 | 3401 | 189.208 | 0.16647 |

| | | | |
|---|---|---|---|
| 0.83 | 3449 | 189.147 | 0.10548 |
| 0.84 | 3499 | 189.1003 | 0.05877 |
| 0.85 | 3550 | 189.0675 | 0.02592 |
| 0.86 | 3604 | 189.048 | 0.00647 |
| 0.87 | 3659 | 189.0415 | 0 |
| 0.88 | 3716 | 189.0476 | 0.00605 |
| 0.89 | 3775 | 189.0657 | 0.02418 |
| 0.9 | 3834 | 189.0955 | 0.05392 |
| 0.91 | 3895 | 189.1364 | 0.09482 |
| 0.92 | 3957 | 189.188 | 0.14642 |
| 0.93 | 4018 | 189.2498 | 0.20827 |
| 0.94 | 2994 | 196.3848 | 7.34321 |
| 0.95 | 4148 | 189.4024 | 0.36088 |
| 0.96 | 4213 | 189.4923 | 0.45076 |
| 0.97 | 4280 | 189.5906 | 0.54909 |
| 0.98 | 2511 | 195.2474 | 6.20584 |
| 0.99 | 4415 | 189.8109 | 0.7694 |
| 1 | 4483 | 189.9321 | 0.89054 |

**Supplementary Table 3**. Left side Pradel model estimates of population growth rate (λ) from configurations supplied with pre-specified survival rates (Phi) from 0.75 to 1 and the associated $AIC_c$ and $\Delta AIC_c$ scores.

| Phi | lambda | AICc | deltaAICc |
|---|---|---|---|
| 0.75 | 1.01 | 1106.373 | 3.5022 |
| 0.76 | 1.014 | 1106.025 | 3.1543 |
| 0.77 | 1.019 | 1105.698 | 2.8272 |
| 0.78 | 1.023 | 1105.392 | 2.5207 |
| 0.79 | 1.027 | 1105.105 | 2.2342 |
| 0.8 | 1.032 | 1104.838 | 1.9675 |
| 0.81 | 1.037 | 1104.591 | 1.7202 |
| 0.82 | 1.042 | 1104.363 | 1.4918 |
| 0.83 | 1.047 | 1104.153 | 1.2819 |
| 0.84 | 1.052 | 1103.961 | 1.09 |
| 0.85 | 1.058 | 1103.787 | 0.9157 |
| 0.86 | 1.063 | 1103.629 | 0.7585 |
| 0.87 | 1.069 | 1103.489 | 0.6177 |
| 0.88 | 1.075 | 1103.364 | 0.493 |
| 0.89 | 1.081 | 1103.255 | 0.3838 |
| 0.9 | 1.087 | 1103.16 | 0.2895 |
| 0.91 | 1.094 | 1103.08 | 0.2095 |
| 0.92 | 1.1 | 1103.014 | 0.1433 |
| 0.93 | 1.107 | 1102.961 | 0.0904 |
| 0.94 | 1.114 | 1102.921 | 0.0501 |

| | | | |
|---|---|---|---|
| 0.95 | 1.12 | 1102.893 | 0.022 |
| 0.96 | 1.128 | 1102.876 | 0.0055 |
| 0.97 | 1.135 | 1102.871 | 0 |
| 0.98 | 1.142 | 1102.876 | 0.005 |
| 0.99 | 1.149 | 1102.891 | 0.02 |
| 1 | 1.157 | 1102.915 | 0.0445 |

**Supplementary Table 4**. Right side Pradel model estimates of population growth rate (λ) from configurations supplied with pre-specified survival rates (Phi) from 0.75 to 1 and the associated $AIC_c$ and $\Delta AIC_c$ scores.

| Phi | lambda | AICc | deltaAICc |
|---|---|---|---|
| 0.75 | 1.05 | 1136.956 | 1.5458 |
| 0.76 | 1.054 | 1136.74 | 1.3293 |
| 0.77 | 1.059 | 1136.541 | 1.1304 |
| 0.78 | 1.063 | 1136.359 | 0.9489 |
| 0.79 | 1.068 | 1136.195 | 0.7844 |
| 0.8 | 1.073 | 1136.047 | 0.6367 |
| 0.81 | 1.078 | 1135.916 | 0.5054 |
| 0.82 | 1.083 | 1135.8 | 0.3902 |
| 0.83 | 1.088 | 1135.701 | 0.2907 |
| 0.84 | 1.093 | 1135.617 | 0.2066 |
| 0.85 | 1.099 | 1135.548 | 0.1373 |
| 0.86 | 1.105 | 1135.493 | 0.0826 |
| 0.87 | 1.11 | 1135.452 | 0.0419 |
| 0.88 | 1.116 | 1135.425 | 0.0149 |
| 0.89 | 1.123 | 1135.411 | 0.0011 |
| 0.9 | 1.129 | 1135.41 | 0 |
| 0.91 | 1.135 | 1135.421 | 0.0112 |
| 0.92 | 1.142 | 1135.444 | 0.0342 |
| 0.93 | 1.149 | 1135.479 | 0.0685 |
| 0.94 | 1.156 | 1135.524 | 0.1137 |
| 0.95 | 1.163 | 1135.58 | 0.1693 |
| 0.96 | 1.17 | 1135.645 | 0.2348 |
| 0.97 | 1.177 | 1135.72 | 0.3098 |
| 0.98 | 1.184 | 1135.804 | 0.3939 |
| 0.99 | 1.192 | 1135.897 | 0.4866 |
| 1 | 1.199 | 1135.998 | 0.5874 |

**Supplementary Table 5**. Derived estimates of annual abundance from the best-fitting (Phi = 0.94, $\Delta AIC_c$ =0) POPAN model for the left-side data.

| yr | estimate | se | lcl | ucl |
|---|---|---|---|---|
| 2004 | 496 | 670 | 67 | 3653 |
| 2005 | 665 | 558 | 159 | 2780 |

| | | | | |
|---|---|---|---|---|
| 2006 | 825 | 468 | 293 | 2323 |
| 2007 | 975 | 407 | 445 | 2138 |
| 2008 | 1116 | 380 | 583 | 2135 |
| 2009 | 1249 | 387 | 689 | 2261 |
| 2010 | 1373 | 422 | 762 | 2474 |
| 2011 | 1490 | 474 | 811 | 2738 |
| 2012 | 1600 | 535 | 846 | 3027 |
| 2013 | 1704 | 599 | 873 | 3327 |
| 2014 | 1801 | 665 | 894 | 3628 |
| 2015 | 1893 | 729 | 913 | 3924 |
| 2016 | 1979 | 792 | 930 | 4212 |
| 2017 | 2059 | 852 | 945 | 4489 |
| 2018 | 2135 | 910 | 959 | 4756 |
| 2019 | 2207 | 965 | 972 | 5010 |

**Supplementary Table 6**. Derived estimates of annual abundance from the best-fitting (lowest $AIC_c$) POPAN model for the right-side data (Phi = 0.87, $\Delta AIC_c$ =0).

| yr | estimate | se | lcl | ucl |
|---|---|---|---|---|
| 2004 | 233 | 633 | 13 | 4059 |
| 2005 | 431 | 481 | 74 | 2512 |
| 2006 | 604 | 368 | 201 | 1815 |
| 2007 | 754 | 300 | 355 | 1599 |
| 2008 | 884 | 283 | 479 | 1632 |
| 2009 | 998 | 306 | 554 | 1797 |
| 2010 | 1096 | 350 | 595 | 2019 |
| 2011 | 1182 | 400 | 620 | 2255 |
| 2012 | 1257 | 450 | 636 | 2483 |
| 2013 | 1322 | 497 | 648 | 2695 |
| 2014 | 1378 | 539 | 658 | 2888 |
| 2015 | 1428 | 577 | 666 | 3061 |
| 2016 | 1470 | 611 | 673 | 3214 |
| 2017 | 1508 | 641 | 679 | 3350 |
| 2018 | 1540 | 667 | 684 | 3470 |
| 2019 | 1568 | 690 | 688 | 3576 |

**Supplementary Table 7**. Derived estimates of annual abundance from the POPAN model for the left-side data when Phi = 0.92 ($\Delta AIC_c$ = 0.044).

| yr | estimate | se | lcl | ucl |
|---|---|---|---|---|
| 2004 | 519 | 672 | 74 | 3632 |
| 2005 | 671 | 554 | 164 | 2755 |
| 2006 | 811 | 459 | 289 | 2279 |
| 2007 | 940 | 393 | 428 | 2066 |
| 2008 | 1059 | 361 | 552 | 2030 |

| | | | | |
|---|---|---|---|---|
| 2009 | 1168 | 363 | 644 | 2117 |
| 2010 | 1268 | 390 | 703 | 2286 |
| 2011 | 1360 | 433 | 740 | 2501 |
| 2012 | 1445 | 484 | 763 | 2738 |
| 2013 | 1523 | 538 | 778 | 2981 |
| 2014 | 1595 | 591 | 790 | 3222 |
| 2015 | 1661 | 643 | 799 | 3456 |
| 2016 | 1722 | 693 | 806 | 3679 |
| 2017 | 1778 | 739 | 813 | 3890 |
| 2018 | 1830 | 783 | 819 | 4089 |
| 2019 | 1877 | 824 | 824 | 4275 |

**Supplementary Table 8**. Derived estimates of annual abundance from the POPAN model for the right-side data when Phi = 0.92 ($\Delta AIC_c$ = 0.146).

| yr | estimate | se | lcl | ucl |
|---|---|---|---|---|
| 2004 | 173 | 601 | 7 | 4005 |
| 2005 | 412 | 471 | 69 | 2473 |
| 2006 | 631 | 374 | 215 | 1850 |
| 2007 | 833 | 323 | 400 | 1733 |
| 2008 | 1018 | 323 | 555 | 1869 |
| 2009 | 1189 | 365 | 661 | 2140 |
| 2010 | 1346 | 428 | 733 | 2472 |
| 2011 | 1491 | 499 | 787 | 2824 |
| 2012 | 1624 | 572 | 831 | 3174 |
| 2013 | 1746 | 643 | 868 | 3513 |
| 2014 | 1859 | 711 | 901 | 3834 |
| 2015 | 1962 | 774 | 931 | 4136 |
| 2016 | 2058 | 834 | 958 | 4419 |
| 2017 | 2145 | 889 | 983 | 4683 |
| 2018 | 2226 | 941 | 1006 | 4928 |
| 2019 | 2300 | 989 | 1026 | 5155 |

**Supplementary Table 9**. Derived estimates of annual abundance from the POPAN model for the left-side data when Phi = 0.99 ($\Delta AIC_c$ = 0.074).

| yr | estimate | se | lcl | ucl |
|---|---|---|---|---|
| 2004 | 448 | 669 | 54 | 3739 |
| 2005 | 657 | 571 | 151 | 2859 |
| 2006 | 864 | 493 | 305 | 2445 |
| 2007 | 1068 | 442 | 490 | 2330 |
| 2008 | 1271 | 429 | 668 | 2419 |
| 2009 | 1472 | 454 | 815 | 2658 |
| 2010 | 1671 | 512 | 929 | 3005 |
| 2011 | 1867 | 591 | 1019 | 3423 |

| | | | | |
|---|---|---|---|---|
| 2012 | 2062 | 685 | 1094 | 3887 |
| 2013 | 2255 | 786 | 1161 | 4380 |
| 2014 | 2446 | 893 | 1223 | 4892 |
| 2015 | 2635 | 1002 | 1282 | 5415 |
| 2016 | 2822 | 1113 | 1339 | 5946 |
| 2017 | 3007 | 1225 | 1395 | 6481 |
| 2018 | 3191 | 1337 | 1450 | 7019 |
| 2019 | 3372 | 1449 | 1505 | 7557 |

**Supplementary Table 10**. Derived estimates of annual abundance from the POPAN model for the right-side data when Phi = 0.99 ($\Delta AIC_c$ = 0.769).

| yr | estimate | se | lcl | ucl |
|---|---|---|---|---|
| 2004 | 112 | 576 | 3 | 3969 |
| 2005 | 398 | 468 | 64 | 2474 |
| 2006 | 681 | 390 | 240 | 1935 |
| 2007 | 961 | 360 | 472 | 1956 |
| 2008 | 1238 | 388 | 679 | 2256 |
| 2009 | 1513 | 462 | 842 | 2716 |
| 2010 | 1784 | 563 | 976 | 3264 |
| 2011 | 2053 | 678 | 1093 | 3858 |
| 2012 | 2320 | 801 | 1202 | 4477 |
| 2013 | 2583 | 927 | 1306 | 5110 |
| 2014 | 2844 | 1055 | 1407 | 5750 |
| 2015 | 3103 | 1184 | 1506 | 6393 |
| 2016 | 3359 | 1314 | 1603 | 7036 |
| 2017 | 3612 | 1443 | 1699 | 7677 |
| 2018 | 3862 | 1571 | 1794 | 8316 |
| 2019 | 4111 | 1699 | 1888 | 8952 |

**Supplementary Table 11**. Derived estimates of annual abundance from the POPAN model for the combined-side data when Phi = 0.92.

| yr | estimate | se | lcl | ucl |
|---|---|---|---|---|
| 2004 | 327 | 448 | 44 | 2453 |
| 2005 | 521 | 359 | 153 | 1767 |
| 2006 | 703 | 290 | 323 | 1529 |
| 2007 | 876 | 250 | 507 | 1515 |
| 2008 | 1036 | 241 | 661 | 1624 |
| 2009 | 1178 | 257 | 772 | 1799 |
| 2010 | 1303 | 288 | 849 | 2000 |

| | | | | |
|---|---|---|---|---|
| 2011 | 1416 | 327 | 906 | 2214 |
| 2012 | 1520 | 369 | 950 | 2431 |
| 2013 | 1615 | 413 | 986 | 2644 |
| 2014 | 1703 | 454 | 1018 | 2848 |
| 2015 | 1784 | 495 | 1046 | 3041 |
| 2016 | 1859 | 533 | 1072 | 3225 |
| 2017 | 1928 | 568 | 1095 | 3395 |
| 2018 | 1992 | 602 | 1116 | 3555 |
| 2019 | 2050 | 633 | 1135 | 3704 |

**Supplementary Table 12**. Derived estimates of annual abundance from the POPAN model for the combined-side data when Phi = 0.99.

| yr | estimate | se | lcl | ucl |
|---|---|---|---|---|
| 2004 | 255 | 437 | 26 | 2526 |
| 2005 | 502 | 362 | 141 | 1784 |
| 2006 | 751 | 306 | 349 | 1619 |
| 2007 | 1004 | 279 | 588 | 1714 |
| 2008 | 1253 | 288 | 803 | 1954 |
| 2009 | 1492 | 324 | 980 | 2272 |
| 2010 | 1722 | 379 | 1125 | 2637 |
| 2011 | 1947 | 446 | 1251 | 3032 |
| 2012 | 2171 | 521 | 1366 | 3451 |
| 2013 | 2392 | 600 | 1475 | 3880 |
| 2014 | 2612 | 682 | 1580 | 4320 |
| 2015 | 2830 | 765 | 1682 | 4762 |
| 2016 | 3046 | 849 | 1782 | 5208 |
| 2017 | 3260 | 934 | 1880 | 5653 |
| 2018 | 3473 | 1018 | 1978 | 6097 |
| 2019 | 3683 | 1102 | 2074 | 6540 |